A 34-Electron Superatom Ag_{78} Cluster with Regioselective Ternary Ligands Shells and Its 2D Rhombic Superlattice Assembly

Wen-Jing Zhang, Zhen Liu, Ke-Peng Song, Christine M. Aikens, Shan-Shan Zhang, Zhi Wang, Chen-Ho Tung, and Di Sun*

Dedicated to the 100th anniversary of Xiamen University.

Abstract: The coverage of surface ligands has important influence on the formation, structure and properties of atomically precise metal nanoclusters. Herein, we report a 78-nuclei silver nanocluster $[Ag_{78}(^{i}PrPhS)_{30}(dppm)_{10}Cl_{10}]^{4+}$ (**SD/Ag78a**; dppm = bis-(diphenyphosphino)methane) that is synthesized by one-pot reaction using $[Ag(pz)]_n$ as precursor (Hpz = pyrazole) and further characterized by X-ray crystallography. **SD/Ag78a** shows a core-shell structure comprised of an all-metallic Ag_{53} kernel surrounded by an Ag_{25} discontinuous metal-organic shell. The Ag_{53} kernel is an Ag_{13} Inodecahedron encaged by an Ag_{40} drum-like shell, while the Ag_{25} shell consists of two $Ag_{10}S_{10}P_{10}Cl_5$ rings and five S-Ag-S staples. Three types of ligands regioselectively cap on the surface of the Ag_{78} nanocluster, forming diverse metal-ligand interfacial structures such as S-Ag-S staples, Cl-capped Ag_3 trigons and S-capped Ag_4 tetragons. This nanocluster is a closed-shell 34-electron superatom with +4 charge state and shows highly featured molecule-like absorption spectra in the ultraviolet-visible region with a maximum around 493 nm. The rhombic superlattice assembled from **SD/Ag78a** through intercluster C-H···π interactions can be formed by a simple drop-casting treatment. This work not only reveals the complicated surface chemistry of silver nanocluster but also provides a promising ternary ligand strategy for the syntheses of them.

Introduction

Ligand-protected atomically precise metal nanoclusters (NCs) have garnered unparalleled attention in the past ten years because of fundamental scientific interest and potential applications based on their fascinating optical, photophysical, electronic, and chemical properties.[1] To acquire precise structure-property correlations, knowledge of the atomically precise structure of NCs is a prerequisite, which thus has driven chemists to synthesize these systems with considerable enthusiasms, in most cases by using diverse protection ligands and controlling the reduction kinetics.[2]

Excepting for the syntheses, the cultivation of high-quality single crystals of such large sized NCs for crystallographic analysis is still a daunting challenge. Since the first X-ray structure of a silver nanoparticle (Ag_{44}) reported in 2013,[3] the Zheng, Wang, Liu, Bakr, Zhu, and Zang groups have augmented this library of silver nanoclusters to some extent by publishing several gorgeous examples such as Ag_{374}, Ag_{22}, Ag_{21}, Ag_{67}, Ag_{62}, and Ag_{14}.[4] Although there have been some advances in the syntheses of ligand passivated NCs, the precise control over the number of metal atoms in kernel, the packing fashion of metal atoms and the surface coordination structures remains a long-sought issue and some detailed ligand effects are still fuzzy.[5] Such circumstances are more pronounced in the silver nanocluster family due to the versatile coordination geometries of silver atoms and their relatively low stability compared to their gold homologues.[6]

Amongst previously reported cases, most silver nanoclusters can be isolated and are amenable to be characterized by the single-crystal X-ray diffraction (SCXRD) technique thanks to protection from organic ligands, which mainly include thiolates, phosphines, and alkynyls, or the combination of two types of ligands. For different kinds of ligands, their bonding preference, stereochemistry and electronics dictate the total structure and properties of silver nanoclusters. In 2018, Zhu group used a pair of isomers of dimethylbenzenethiolates (2,4- and 2,5-dimethylbenzenethiolate, abbreviated as 2,4-DMBT or 2,5-DMBT) in the presence of triphenylphosphine (Ph_3P) to isolate a pair of unique silver nanoclusters, $[Ag_{40}(2,4\text{-}DMBT)_{24}(PPh_3)_8]$ and $[Ag_{46}(2,5\text{-}DMBT)_{24}(PPh_3)_8]$, which have clearly exemplified the ligand effects on the core structures and the optical properties.[7] Smaller halogen anions (Cl^-, Br^- and I^-) also exhibit passivation/protection effects on the metal nanoclusters in spite of not being frequently observed.[8] Zheng group has reported a giant Ag_{141} cluster co-protected by 40 adamantanethiolate and 12 Cl^-, Br^- or I^-,[9] from which some interesting Br-Ag polygonal interfacial motifs were observed.

Based on the above considerations, we are very curious about how ternary ligands influence the formation and structure of silver nanoclusters and whether they produce unique arrangements/motifs on the surface. To the best of our knowledge, the only two pure silver nanoclusters built by ternary ligands to date are $[Ag_{32}(SAdm)_{13}(dppm)_5Cl_8]^{3+}$, $[Ag_{45}(SBu^{t})_{16}(dppm)_4Br_{12}]^{3+}$ (SAdm = 1-adamantanethiolate), however, no special ligand distribution can be observed in

[*] W.-J. Zhang, S.-S. Zhang, Dr. K.-P. Song, Z. Wang, Prof. C.-H. Tung, Prof. D. Sun
Key Lab of Colloid and Interface Chemistry, Ministry of Education, School of Chemistry and Chemical Engineering, State Key Laboratory of Crystal Materials, Shandong University, Ji'nan, 250100, P. R. China
E-mail: dsun@sdu.edu.cn
Z. Liu, Prof. C. M. Aikens
Department of Chemistry, Kansas State University, Manhattan, Kansas 66506, USA.
Supporting information for this article is available on the WWW under http://dx.doi.org/10.1002/anie.201xxxxxx.

these systems, which prevented us from understanding the respective ligand effect.[10]

In this work, we demonstrate that the combination of three kinds of ligands, thiol, phosphine and chloride, can facilitate the formation of ternary ligand co-protected silver nanocluster. Specifically, using ^{i}PrPhS^{-}, dppm and Cl^{-}, a silver nanocluster, $[Ag_{78}(^{i}PrPhS)_{30}(dppm)_{10}Cl_{10}]^{4+}$, was isolated. It has a double-shell $Ag_{13}@Ag_{40}$ kernel protected by a shell of $[Ag_{25}(^{i}PrPhS)_{30}(dppm)_{10}Cl_{10}]$, which is composed of two $Ag_{10}S_{10}P_{10}Cl_5$ rings and five S-Ag-S staples. Three different ligands regioselectively ligate on the surface of the Ag_{78} nanocluster, forming multiple metal-ligand interfacial structures such as S-Ag-S staples, Cl-capped Ag_3 trigons and S-capped Ag_4 tetragons, which dictate the final structure of **SD/Ag78a**.

Scheme 1. Synthetic Route for **SD/Ag78a**. (dppm = bis-(diphenyphosphino)methane and Hpz = pyrazole)

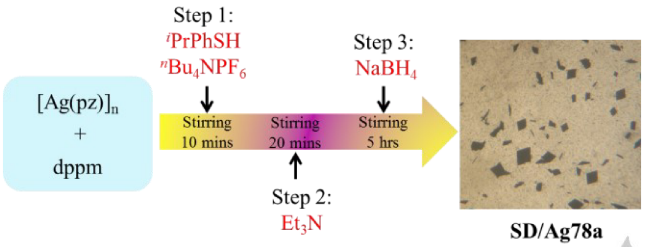

Results and Discussion

Synthesis Discussion

SD/Ag78a was synthesized by a facile one-pot reaction in a mixed solvent system of $CHCl_3$/CH_3CN/EtOH at room temperature using a simple silver coordination polymer, $[Ag(pz)]_n$ (Hpz = pyrazole),[11] as precursor (Scheme 1). The purity of it has been verified by powder X-ray diffraction (PXRD, Figure S1). The black plate crystals were collected as bulk sample after evaporation of solvents of mother liquor at room temperature for about ten days. The source of Cl^{-} should be from $CHCl_3$ by in situ decomposition, which is a common phenomenon in the assembly of silver nanoclusters.[12] If using a non-chlorinated solvent, **SD/Ag78a** cannot be isolated in the similar synthesis system. Intentionally adding NaCl as a Cl^{-} source will not increase the yield of **SD/Ag78a**. We did not add any other silver salt, so the insoluble $[Ag(pz)]_n$ is the sole source for Ag^{+} ions. The release of Ag^{+} ion from insoluble $[Ag(pz)]_n$ is quite slow, which thus slows down the reduction reaction speed in the presence of $NaBH_4$, then facilitates to from high-quality crystals of **SD/Ag78a**. Although the pz^{-} ligand does not participate in the structure of **SD/Ag78a**, its strong coordination effect makes $[Ag(pz)]_n$ as an Ag^{+} ions slow-release source to realize the assembly of **SD/Ag78a**. If other silver salts such as AgOAc, CF_3COOAg, CF_3SO_3Ag, $AgBF_4$, AgCl, AgBr, and $AgNO_3$ are used as the silver source, we cannot obtain **SD/Ag78a**. Apart from single-crystal X-ray diffraction (SCXRD), **SD/Ag78a** was thoroughly characterized by infrared spectroscopy (IR), ultraviolet-visible (UV-Vis) spectroscopy, PXRD, and energy dispersive spectroscopy (EDS). These characterizations, additional structural graphics, as well as crystallography related information are collected in the Supporting Information (SI, Figure S2-S18, Table S1-S3). Moreover, density functional theory (DFT) calculations were also performed to understand the electronic structure and optical properties (SI, Figure S19 and S20, Table S4 and S5).

X-Ray Structure of SD/Ag78a

Single-crystal X-ray crystallographic analysis at 100 K revealed that **SD/Ag78a** crystallized in an orthorhombic lattice with a space group of *P*bcn (Schoenflies: D_{2h}^{14}) with *a* = 34.7898(4), *b* = 40.6911(6) and *c* = 43.5436(4) Å (Table S1). Only a half of the cluster is found in the asymmetric unit due to the coincident 2-fold axis with the cluster along the *b* direction, which passes through Ag6, Ag8, Ag34 and Ag39. The total composition of **SD/Ag78a** is determined to be $[Ag_{78}(^{i}PrPhS)_{30}(dppm)_{10}Cl_{10}]\cdot 2dppmO_2\cdot 4PF_6\cdot 2MeCN$.

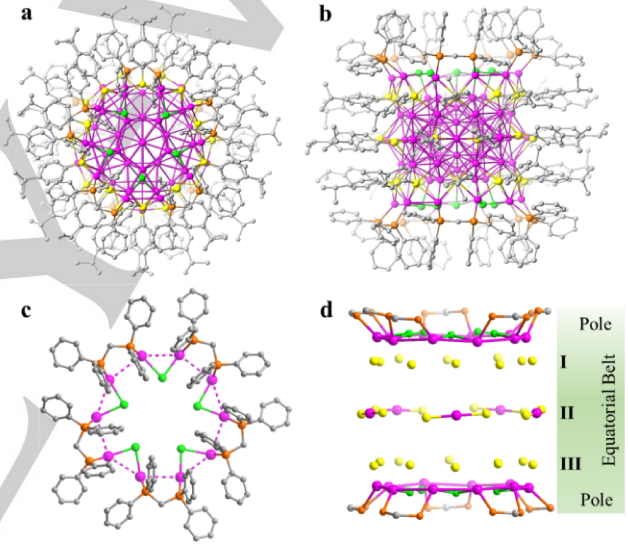

Figure 1. Top (a) and side (b) views of the total molecular structure of **SD/Ag78a**. Hydrogen atoms are removed for clarity. (c) Top view of a $Ag_{10}(dppm)_5Cl_5$ ring. (d) The complete Ag_{25} metal-organic shell showing regioselective distribution of ternary ligands. Phenyl rings and ^{i}PrPh groups are removed from the ligands for clarity. Color legend: Ag, purple; S, yellow; P, orange; Cl, green; C, gray.

SD/Ag78a exhibits a quasi-D_{5h} symmetry and roughly barrel-like geometry (Figure 1a and 1b) with a dimension of 1.1 × 1.1 nm excluding the ligand shell. For a more comprehensive anatomy of this cluster, we analyzed the structure starting from the outer metal-ligand shell to the inner Ag_{53} core. The ligand shell contains 30 ^{i}PrPhS^{-}, 10 dppm and 10 Cl^{-} which cover the surface of **SD/Ag78a**. Interestingly, they selectively cap on the two poles or the equatorial belt instead of in an arbitrary fashion. In detail, five μ_2-dppm and five μ_3-Cl^{-} ligands are distributed on each pole in a pentagonal arrangement and synergistically bind ten silver atoms to form a $Ag_{10}(dppm)_5Cl_5$ ring (Ag-Cl: 2.49-2.78 Å; Ag-P: 2.38-2.40 Å; Figure 1c). All pentagons on the two poles built from five dppm or five Cl^{-} ligands are located in an eclipsed configuration (Figure S2a). It is also interesting to find that a CH_3CN molecule resides in the cavity of the

$Ag_{10}(dppm)_5Cl_5$ ring and is fixed by nonclassical C-H···Cl hydrogen bonds (C···Cl: 3.60-3.69 Å; Figure S2b). There are three layers (**I-III**) of the $^{i}PrPhS^{-}$ ligand arrays on the equatorial belt and each layer contains ten $^{i}PrPhS^{-}$ ligands (Figure 1d). Ten $^{i}PrPhS^{-}$ ligands in layer **II** bind five silver atoms to form five S-Ag-S staples (Ag-S: 2.32-2.34 Å; Figure S3), whereas the $^{i}PrPhS^{-}$ ligands in layers **I** and **III** mainly connect $Ag_{10}(dppm)_5Cl_5$ rings and the inner Ag_{53} kernel using a μ_4 mode (Ag-S: 2.55-2.74 Å; Figure S4). All of these components constitute the outer Ag_{25} discontinuous metal-organic shell (3rd shell) where the shortest Ag···Ag contact is near to the upper limit of the defined argentophilic interaction distance (< 3.44 Å);[13] thus, almost no Ag···Ag interactions can be observed in the Ag_{25} outer shell.

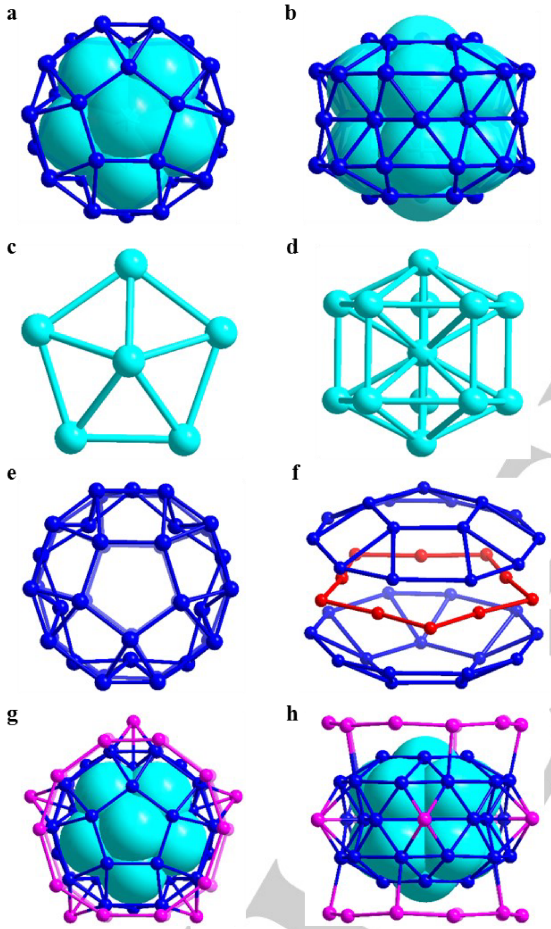

Figure 2. Top (a) and side (b) views of double-shell Ag_{53} kernel. The inner Ag_{13} Inodecahedron is shown in space-filling mode. Top (c) and side (d) views of inner Ag_{13} Inodecahedron. (e) The 2nd Ag_{40} shell viewed along the top pentagon. (f) Two pentagonal cupola (J_5) sandwiching an Ag_{10} pentagon (red ring) in Ag_{40} shell. Top (g) and side (h) views of the overall metallic framework of **SD/Ag78a**. All colored balls are silver atoms but discriminated based on which shells they are located in.

Under the Ag_{25} metal-organic shell is a double-shell kernel of 53 silver atoms (Figure 2a and 2b) which is built from the concentric 1st Ag_{13} and 2nd Ag_{40} shell. The thirteen innermost silver atoms are arranged in the form of an Inodecahedron (1st Ag_{13} shell) which can be seen as two Ag_7 pentagonal bipyramids (also called decahedra) packed in an eclipsed configuration (Figure 2c and 2d) by sharing a vertex silver atom (Ag6). The Ag6 atom forms a 12-fold coordination with the 12 surface Ag atoms. The average Ag···Ag distance from Ag6 to the vertexes of the Ag_{13} Inodecahedron is 2.94 Å, and the average Ag···Ag distance on the surface of the Inodecahedron (Ag_{13}) is 2.95 Å, both of which are slightly longer than the 2.88 Å bond length in elemental silver.[14] Similar single Ag_7 decahedral units and vertex-fused Ag_7 decahedra have been observed in large silver nanoclusters such as Ag_{141}, Ag_{146}, Ag_{206} and Ag_{210},[9,15] but the packing configuration of the Ag_7 units varies from staggered to eclipsed.

Around the Inodecahedral Ag_{13} core, there are another 40 silver atoms (Figure 2e), which make a drum-like shell with two Ag_{15} pentagonal cupola (J_5)[16] as caps sandwiching an Ag_{10} pentagon (Figure 2f). Two Ag_{15} pentagonal cupola (J_5) are in an eclipsed configuration but rotated by 36.7° with respect to the equatorial Ag_{10} pentagon. The interatomic distances in this shell span from 2.79 to 3.17 Å which are still in the range of argentophilic interactions. The Ag···Ag distances between the 1st Ag_{13} and 2nd Ag_{40} shell are in the range of 2.75-2.96 Å. This Ag_{40} shell further interacts with the outermost 3rd Ag_{25} segment through Ag···Ag interactions (2.90-3.44 Å) to form the overall 78-nuclei metallic framework of **SD/Ag78a** (Figure 2g and 2h). The shell-by-shell analysis of the Ag···Ag distances in **SD/Ag78a** is shown in Figure S5 and the averaged value in each shell shows a regular trend from inner to outer: 2.95 Å^{1st} < 2.98 Å^{2nd} < 3.44 Å^{3rd}.

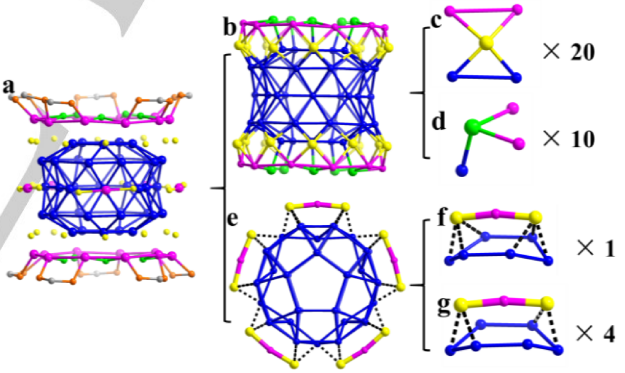

Figure 3. The anatomy of the surface coordination structures in **SD/Ag78a**. (a) The outmost Ag_{25} metal-organic shell enwrapping the Ag_{40} shell in the core. (b) The capping of $Ag_{10}(dppm)_5Cl_5$ rings on the Ag_{40} shell at two poles by forming 20 Ag_4-S tetragons (c) and 10 Ag_3-Cl trigons (d). (e) Five S-Ag-S staples surrounding the equatorial region of the Ag_{40} shell with different binding fashions (f) and (g). Color legend: Ag, purple and blue; S, yellow; P, orange; Cl, green; C, gray.

Another fascinating feature of **SD/Ag78a** lies in the diverse interfacial coordination structures benefitting from the usage of the ternary ligand system (Figure 3a). At each pole, the $Ag_{10}(dppm)_5Cl_5$ ring connects with the 2nd Ag_{40} shell (Figure 3b) through forming ten edge-sharing S-capped Ag_4 tetragons (Figure 3c), where the S atom exclusively adopts a quadruple binding fashion to bridge two silver atoms from the Ag_{40} shell and another two from the $Ag_{10}(dppm)_5Cl_5$ ring. In the same region, we also observed five Cl-capped Ag_3 trigons comprising two silver atoms from the $Ag_{10}(dppm)_5Cl_5$

ring and the other from the Ag_{40} shell (Figure 3d). Five S-Ag-S staples embrace the equatorial region of the Ag_{40} shell (Figure 3e) and anchor on it through binding a pair of Ag_3 or Ag_2 units (Figure 3f and 3g). The bond angles of S-Ag-S staples range from 168.52 to 170.01°, indicating their approximately linear configuration as observed in a classic S-Au-S staple.[17]

We also noted a pair of $dppmO_2$ molecules residing in a void formed by six clusters in one unit cell (Figure S6). The existence of $dppmO_2$ in **SD/Ag78a** can be also confirmed by IR spectrum which shows a typical P=O stretching vibration peak at 1190 cm^{-1} (Figure S7).[18] It is well known that the aerobic oxidation of phosphines such as Ph_3P and dppm is a slow process[19] and the purity of dppm used in this system was proven by ^{31}P NMR (Figure S8). If silver salt is removed from the synthesis system, no $dppmO_2$ can be observed in the ^{31}P NMR spectrum even in the presence of O_2 (Figure S8). Thus, the dppm should be *in situ* oxidized by O_2 in the presence of the Ag^I ion.[4, 20]

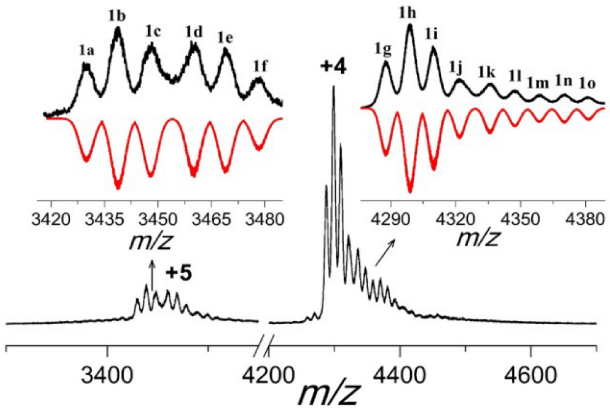

Figure 4. Positive-ion mode ESI-MS of the crystals of **SD/Ag78a** dissolved in CH_2Cl_2. Insets: Zoom-in ESI-MS of experimental (black line) and simulated (red line) for each labeled species.

Mass Spectrometry of SD/Ag78a

As we know, electrospray ionization mass spectrometry (ESI-MS) is a very powerful tool to determine the chemical composition and charge state of metal clusters.[21] The positive-ion ESI-MS of **SD/Ag78a** was measured by dissolving it in dichloromethane, ethanol and acetonitrile, respectively (Figure S9), which exhibit quite similar signals. As a representative, we only discuss the ESI-MS in dichloromethane in detail below. As shown in Figure 4, there are two grouped peaks in the mass-to-charge (*m/z*) ratios ranges of 3400-3500 and 4200-4400, respectively. Expanding each peak gives characteristic differences between two adjacent peaks in the isotopic distribution; these are 0.2 and 0.25, which correspond to +5 and +4 species, respectively. In total, six +5 (**1a**-**1f**) and nine +4 (**1g**-**1o**) species were identified based on the perfect matching of observed and simulated isotopic distributions. All these assigned formulas were listed in Table S3, which show that all of them contain complete 78-nuclei silver framework, indicating the high stability of this cluster in dichloromethane. We also observed slight disassociation of ligands from the surface of cluster. It should be noted that the most dominant peak (**1h**) is located at 4298.7656 and assigned to $[Na_2Ag_{78}(^iPrPhS)_{30}(dppm)_{10}Cl_{10}]^{4+}$ (Calcd. 4298.7995), which is parent cluster but with two sodium attachment **[SD/Ag78a**+2Na$]^{4+}$. It is clear that the **SD/Ag78a** is a +4 cluster compensated by four guest PF_6^- anions in solid state as revealed by SCXRD. However, the existence of **1h** suggests that the charge state of the Ag_{78} cluster changes to +2 during the ESI-MS data collection. Such phenomenon has also observed in several other metal nanoclusters such as in Ag_{44}, Ag_{40}, Ag_{112} and Au_{18}.[3, 7, 22] Anyway, all other 14 species excepting for **1h** can directly or indirectly evidence the +4 charge state of **SD/Ag78a**.

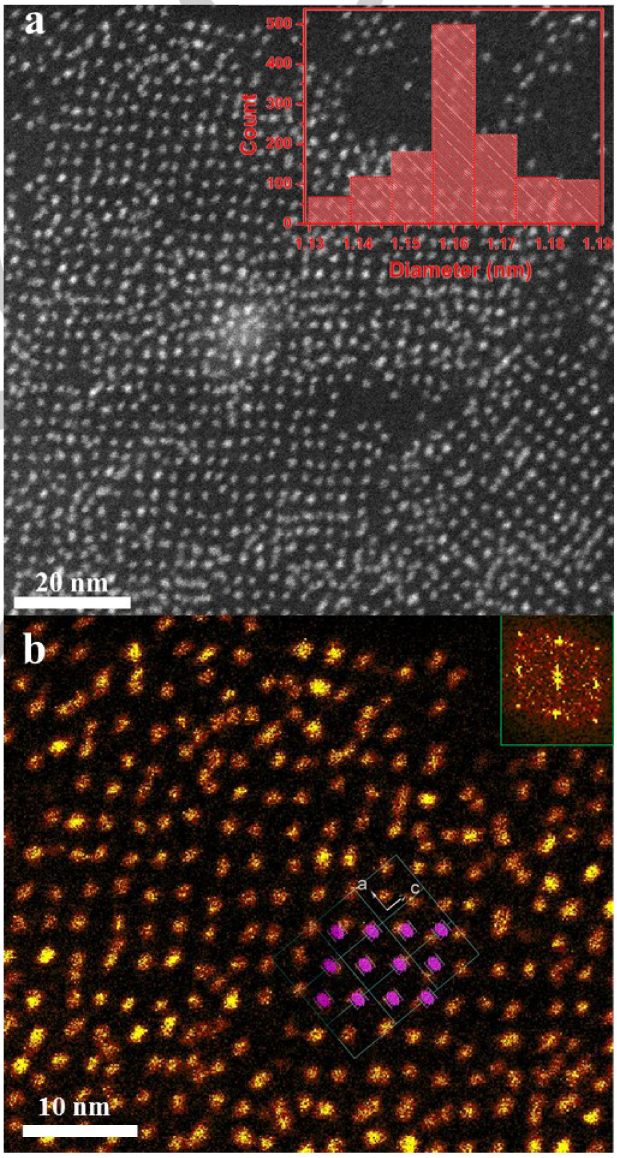

Figure 5. (a) HAADF-STEM image of Ag_{78} cluster. Inset: Size distribution of the Ag_{78} clusters. (b) Zoom-in HAADF-STEM image in Figure 5a and fast Fourier transform (inset on top right corner) of a rhombic superlattice monolayer self-assembled from Ag_{78} clusters. The lower right inset shows well superimposed 2D layer of Ag_{78} cluster in *ac* crystallographic plane with partial nanoparticles in HAADF-STEM image.

Two-Dimensional Superlattices Assembly from SD/Ag78a

The stability of Ag_{78} cluster in dichloromethane solution was also convinced by high-angle annular dark-field scanning transmission electron microscopy (HAADF-STEM) which showed a very tight cluster-size distribution with an average diameter at ~ 1.16 nm, quite similar to the metallic core size of Ag_{78} cluster (1.1 nm) determined by SCXRD (Figure 5a). More interesting, when we carefully checked the arrangement of Ag_{78} cluster on the carbon membrane (Figure 5b), a rhombic superlattice is formed by means of solvent-drying-induced assembly at room temperature.[23] The nearest cluster-to-cluster distances along two directions of rhombic array are estimated to be 2.9 and 2.6 nm, respectively, which are comparable to those found in two-dimensional (2D) cluster (~ 2.8 nm) packing along crystallographic *ac* plane. By analyzing the inter-cluster interactions based on SCXRD results, we found that the C-H···π interactions (Figure S10) between dppm ligands on adjacent clusters exist within crystallographic *ac* plane, which dictates the 2D rhombic superlattice assembly of Ag_{78} cluster on this plane. More important, the regioselective arrangement of $^{i}PrPhS^{-}$ and dppm also decides the preferred orientation when forming array. Although many colloidal nanoparticles have been ordered into superlattice,[24] the nanocluster with atomically precise structure has rarely been used to fabricate 2D superlattice.

Optical and Electrochemical Properties

The solution formed by dissolving **SD/Ag78a** in ethanol appears brown. The optical absorption spectrum of **SD/Ag78a** presented in Figure 6a manifests structured molecule-like multiple peaks tailing to 900 nm. The multiband optical absorption comprises of a sharp peak at 493 nm (2.52 eV) along with four shoulder peaks before and after it at 373, 439, 557 and 602 nm, respectively. The optical energy gap is determined to be 1.12 eV (Figure 6a, inset). The absorption spectra of **SD/Ag78a** dissolved in other solvents such as dichloromethane and acetonitrile show quite similar feature to that in ethanol (Figure S11a). The Ag_{78} nanocluster can keep stable in EtOH for at least two days as revealed by monitored UV-Vis spectra and ESI-MS (Figure S11b and 11c). Based on SCXRD analysis, **SD/Ag78a** is a quadruply charged cationic cluster with 34 free valence electrons (34 = 78 (Ag)-30 (SR)-10 (Cl)-4 (z)), which can be described in a jellium model[25] of $1S^{2}1P^{6}1D^{10}2S^{2}1F^{14}$. This free electron count falls in the "magic" number series (2, 8, 18, 20, 34, 40, 58, 68,...),[26] so **SD/Ag78a** forms a closed electronic shell and is quite stable.[27] Zheng group also reported a 78-nuclei silver nanocluster co-protected by chiral diphosphines and thiols but possessing 36 free electrons,[28] which thus showed a completely different UV-Vis profile (λ_{abs}^{max} = 528 nm) compared to that of **SD/Ag78a**. The comparative results show that the electron count plays an important role in determining the optical properties of silver nanoclusters.

The electrochemical behavior of **SD/Ag78a** was studied in 0.1 M $^{n}Bu_4NPF_6$-CH_2Cl_2 at -5 °C using differential pulse voltammetry (DPV) measurement (Figure 6b). The result shows that two reduction peaks locate at -0.88 (R1) and -1.31 V (R2) and one oxidation peak at 0.16 V (O1). The electrochemical HOMO−LUMO gap obtained from potential difference between the first oxidation and reduction peaks without subtracting the charging energy is 1.04 eV, which is similar to that derived from optical gap (1.12 eV).[29]

To further understand the electronic structure of **SD/Ag78a**, we have tried to perform DFT calculations on **SD/Ag78a** in the +2 and +4 charge state (see more details in SI). However, only $[Ag_{78}(^{i}PrPhS)_{30}(dppm)_{10}Cl_{10}]^{4+}$ with 34 free electrons converged with a large HOMO-LUMO gap (0.68 eV), which further confirmed the genuine charge state of **SD/Ag78a** to be +4 as revealed by SCXRD.

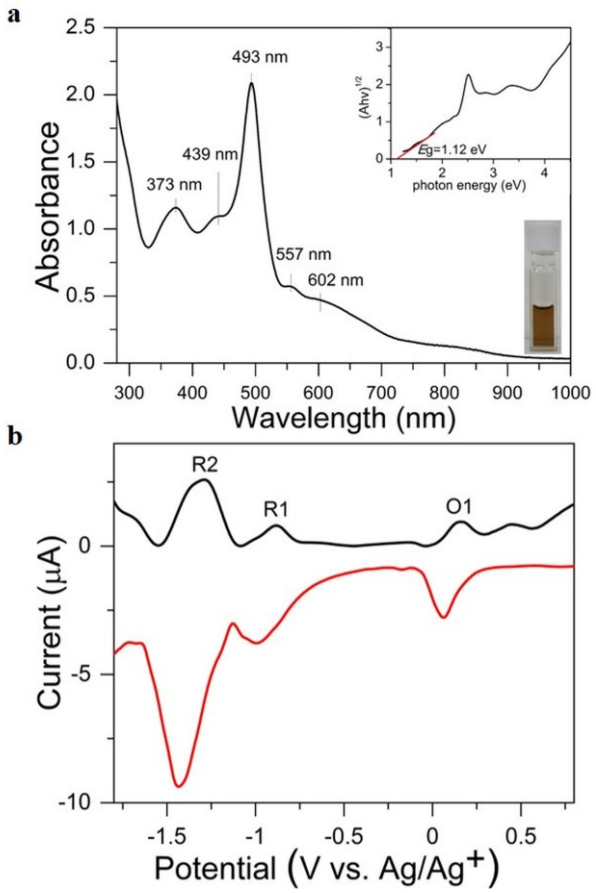

Figure 6. (a) Optical absorption spectra of **SD/Ag78a** dissolved in EtOH. Inset (right bottom): Photograph of crystals dissolved in EtOH. Inset (right top): Spectrum on the energy scale (eV). (b) DPV of **SD/Ag78a** dissolved in CH_2Cl_2 containing 0.1 M $^{n}Bu_4NPF_6$ as electrolyte.

Conclusion

In summary, we have synthesized a ternary ligand co-protected Ag_{78} nanocluster starting from a simple silver coordination polymer as a precursor and determined its structure at atomic precision. This cluster has a core-shell structure featuring a brand-new Ag_{53} kernel enwrapped by an Ag_{25} discontinuous metal-organic shell. The Ag_{53} kernel can be understood in a shell-by-shell fashion with an Ag_{13} Inodecahedron encaged by an Ag_{40} shell. Three types of

ligands of thiol, phosphine and chloride regioselectively ligate on the surface of the Ag_{78} nanocluster, forming rich metal-ligand interfacial structures including S-Ag-S staples, Cl-capped Ag_3 trigons and S-capped Ag_4 tetragons. This nanocluster has a jelliumatic electron count of 34 and shows molecule-like absorption behavior. Orbitals near the HOMO-LUMO gap are primarily composed of 5sp electrons from Ag, but the strong excitation in the optical absorption spectrum arises from transitions from the ^{i}PrPhS^{-} ligands into the silver core. This nanocluster with atomically precise structure has been fabricated 2D superlattice for the first time, which illustrates how the detailed intercluster interactions influence the final structure of superlattice. This work not only reveals complicated surface chemistry of silver nanocluster but also provides a promising ligand strategy for the synthesis of it and further superlattice assembly.

Acknowledgements

This work was financially supported by the National Natural Science Foundation of China (Grant Nos. 91961105, 21822107, 21571115, 21827801), the Natural Science Foundation of Shandong Province (Nos. ZR2019ZD45, JQ201803 and ZR2017MB061), and the Taishan Scholar Project of Shandong Province of China (Nos. tsqn201812003 and ts20190908). Project for Scientific Research Innovation Team of Young Scholar in Colleges and Universities of Shandong Province (2019KJC028). Z. L. and C. M. A were supported by the National Science Foundation (CHE-1905048) of the United States. The computing for this work was performed on the Beocat Research Cluster at Kansas State University, which is funded in part by NSF grants CHE-1726332, CNS-1006860, EPS-1006860, and EPS-0919443. We thank Y. Z. Tan (Xiamen University), G. L. Zhuang (Zhejiang University of Technology), Z. J. Yang and J. H. Zhan (Shandong University) for helpful discussions.

Keywords: core-shell structure • silver nanocluster • regioselective coverage • superlattice assembly

[1] a) M. Agrachev, M. Ruzzi, A. Venzo, F. Maran, *Acc. Chem. Res.* **2019**, *52*, 44-52; b) C. M. Aikens, *Acc. Chem. Res.* **2018**, *51*, 3065-3073; c) M. Zhou, C.-J. Zeng, Y.-B. Song, J. W. Padelford, G.-L. Wang, M. Y. Sfeir, T. Higaki, R.-C. Jin, *Angew. Chem. Int. Ed.* **2017**, *56*, 16257-16261; d) A. W. Cook, T. W. Hayton, *Acc. Chem. Res.* **2018**, *51*, 2456-2464; e) K. Konishi, *Struct. Bond.* **2014**, *161*, 49-86; f) N. A. Sakthivel, A. Dass, *Acc. Chem. Res.* **2018**, *51*, 1774-1783; g) Q.-F. Zhang, X.-N. Chen, L.-S. Wang, *Acc. Chem. Res.* **2018**, *51*, 2159-2168; h) G. Li, R.-C. Jin, *Acc. Chem. Res.* **2013**, *46*, 1749-1758; i) H.-F. Qian, M.-Z. Zhu, Z.-K. Wu, R.-C. Jin, *Acc. Chem. Res.* **2012**, *45*, 1470-1479.

[2] a) P. Chakraborty, A. Nag, A. Chakraborty, T. Pradeep, *Acc. Chem. Res.* **2019**, *52*, 2-11; b) Z.-B. Gan, N. Xia, Z.-K. Wu, *Acc. Chem. Res.* **2018**, *51*, 2774-2783; c) R.-C. Jin, C.-J. Zeng, M. Zhou, Y.-X. Chen, *Chem. Rev.* **2016**, *116*, 10346-10413.

[3] a) H.-Y. Yang, Y. Wang, H.-Q. Huang, L. Gell, L. Lehtovaara, S. Malola, H. Hakkinen, N.-F. Zheng, *Nat. Commun.* **2013**, *4,* 2422; b) A. Desireddy, B. E. Conn, J.-S. Guo, B. Yoon, R. N. Barnett, B. M. Mnahan, K. Kirschbaum, W. P. Griffith, R. L. Whetten, U. Landman, T. P. Bigioni, *Nature* **2013**, *501*, 399-402.

[4] a) H.-Y. Yang, Y. Wang, X. Chen, X.-J. Zhao, L. Gu, H.-Q. Huang, J.-Z. Yan, C. F. Xu, G. Li, J.-C. Wu, A. J. Edwards, B. Dittrich, Z.-C. Tang, D.-D. Wang, L. Lehtovaara, H. Hakkinen, N.-F. Zheng, *Nat. Commun.* **2016**, *7*, 12809; b) S.-F. Yuan, Z.-J. Guan, W.-D. Liu, Q.-M. Wang, *Nat. Commun.* **2019**, *10*, 4032; c) R. S. Dhayal, J.-H. Liao, Y.-C. Liu, M.-H. Chiang, S. Kahlal, J. Y. Saillard, C. W. Liu, *Angew. Chem. Int. Ed.* **2015**, *54*, 3702-3706; d) M. J. Alhilaly, M. S. Bootharaju, C. P. Joshi, T. M. Besong, A. H. Emwas, R. Juarez-Mosqueda, S. Kaappa, S. Malola, K. Adil, A. Shkurenko, H. Hakkinen, M. Eddaoudi, O. M. Bakr, *J. Am. Chem. Soc.* **2016**, *138*, 14727-14732; e) S. Jin, S.-X. Wang, Y.-B. Song, M. Zhou, J. Zhong, J. Zhang, A.-D. Xia, Y. Pei, M. Chen, P. Li, M.-Z. Zhu, *J. Am. Chem. Soc.* **2014**, *136*, 15559-15565; f) Z.-Y. Wang, M.-Q. Wang, Y.-L. Li, P. Luo, T.-T. Jia, R.-W. Huang, S.-Q. Zang, T. C. W. Mak, *J. Am. Chem. Soc.* **2018**, *140*, 1069-1076.

[5] a) I. Chakraborty, T. Pradeep, *Chem. Rev.* **2017**, *117*, 8208-8271; b) X. Kang, M.-Z. Zhu, *Small* **2019**, *15*, 1902703.

[6] J. Yang, R. Jin, *ACS Materials Letters* **2019**, *1*, 482-489.

[7] J.-S. Chai, S. Yang, Y. Lv, T. Chen, S.-X. Wang, H.-Z. Yu, M.-Z. Zhu, *J. Am. Chem. Soc.* **2018**, *140*, 15582-15585.

[8] B. K. Teo, K. Keating, *J. Am. Chem. Soc.* **1984**, *106*, 2224-2226.

[9] L. T. Ren, P. Yuan, H.-F. Su, S. Malola, S.-C. Lin, Z.-C. Tang, B. K. Teo, H. Hakkinen, L.-S. Zheng, N.-F. Zheng, *J. Am. Chem. Soc.* **2017**, *139*, 13288-13291.

[10] X. J. Zou, S. Jin, W.-J. Du, Y.-F. Li, P. Li, S.-X. Wang, M.-Z. Zhu, *Nanoscale* **2017**, *9*, 16800-16805.

[11] N. Masciocchi, M. Moret, P. Cairati, A. Sironi, G. A. Ardizzoia, G. L. Monica, *J. Am. Chem. Soc.***1994**, *116*, 7668-7676.

[12] S. D. Bian, Q.-M. Wang, *Chem. Commun*. **2008**, 5586-5588.

[13] a) H. Schmidbaur, A. Schier, *Angew. Chem. Int. Ed.* **2015**, *54*, 746-784; b) P. Pyykkö, *Chem. Rev.* **1997**, *97*, 597-636.

[14] S. Sculfort, P. Braunstein, *Chem. Soc. Rev.* **2011**, *40*, 2741-2760.

[15] a) Y.-B. Song, K. Lambright, M. Zhou, K. Kirschbaum, J. Xiang, A.-D. Xia, M.-Z. Zhu, R.-C. Jin, *ACS Nano*. **2018**, *12*, 9318-9325; b) J.-Y. Liu, F. Alkan, Z. Wang, Z.-Y. Zhang, M. Kurmoo, Z. Yan, Q.-Q. Zhao, C. M. Aikens, C.-H. Tung, D. Sun, *Angew. Chem. Int. Ed.* **2019**, *58*, 195-199; c) J.-Z. Yan, J. Zhang, X.-M. Chen, S. Malola, B. Zhou, E. Selenius, X.-M. Zhang, P. Yuan, G.-C. Deng, K.-L. Liu, H.-F. Su, B. K. Teo, H. Häkkinen, L.-S. Zheng, N.-F. Zheng, *Natl Sci Rev,* **2018**, *5*, 694-702.

[16] a) N. W. Johnson, *Can. J. Math.* **1966**, *18*, 169-200; b) Z. Wang, H.-F. Su, X.-P. Wang, Q.-Q. Zhao, C.-H. Tung, D. Sun, L.-S. Zheng, *Chem. Eur. J.* **2018**, *24*, 1640-1650.

[17] a) E. Pensa, E. Cortes, G. Corthey, P. Carro, C. Vericat, M. H. Fonticelli, G. Benitez, A. A. Rubert, R. C. Salvarezza, *Acc. Chem. Res.* **2012**, *45*, 1183-1192; b) P. D. Jadzinsky, G. Calero, C. J. Ackerson, D. A. Bushnell, R. D. Kornberg, *Science* **2007**, *318*, 430-433.

[18] F. Marchetti, C. Pettinari, A. Pizzabiocca, A. A. Drozdov, S. I. Troyanov, C. O. Zhuravlev, N. S. Semenov, Y. A. Belousov, I. G. Timokhin, *Inorg. Chim. Acta.* **2010**, *363*, 4038-4047.

[19] A. Loas, S. M. Gorun, *Eur. J. Inorg. Chem.* **2016**, 2648-2657.

[20] A. Belyaev, T. M. Dau, J. Janis, E. V. Grachova, S. P. Tunik, I. O. Koshevoy, *Organometallics* **2016**, *35*, 3763-3774.

[21] a) T. Chen, Q. Yao, R. R. Nasaruddin, J. Xie, *Angew. Chem. Int. Ed.* **2019**, *58*, 11967-11977; b) K. R. Krishnadas, A. Ghosh, A. Baksi, I. Chakraborty, G. Natarajan, T. Pradeep, *J. Am. Chem. Soc.* **2016**, *138*, 140-148; c) A. Nag, P. Chakraborty, G. Paramasivam, M. Bodiuzzaman, G. Natarajan, T. Pradeep, *J. Am. Chem. Soc.* **2018**, *140*, 13590-13593; d) W.-M. Xuan, A. J. Surman, Q. Zheng, D.-L. Long, L. Cronin, *Angew. Chem. Int. Ed.* **2016**, *55*, 12703-12707; e) W.-M. Xuan, A. J. Surman, H. N. Miras, D.-L. Long, L. Cronin, *J. Am. Chem. Soc.* **2014**, *136*, 14114-14120.

[22] a) F. Hu, J.-J. Li, Z.-J. Guan, S.-F. Yuan, Q.-M. Wang, *Angew. Chem. Int. Ed.* **2020**, *59*, 5312-5315; b) S.-S. Zhang, R. D. Senanayake, Q.-Q. Zhao, H.-F. Su, C. M. Aikens, X.-P. Wang, C.-H. Tung, D. Sun, L.-S. Zheng, *Dalton Trans.* **2019**, *48*, 3635.

[23] a) M. A. Boles, M. Engel, D. V. Talapin, *Chem Rev.* **2016**, *116*, 11220-11289; b) J. J. Geuchies, C. V. Overbeek, W. H. Evers, B. Goris, A. D. Backer, A. P. Gantapara, F. T. Rabouw, J. Hilhorst, J. L. Peters, O. Konovalov, A. V. Petukhov, M. Dijkstra, L. D. Siebbeles, S. V. Aert, S. Bals, D. Vanmaekelbergh, *Nat. Mater.* **2016**, *15*, 1248–1254; c) C. B. Murray, C. R. Kagan, M. G. Bawendi, *Annu. Rev. Mater. Sci.* **2000**, *30*, 545-610.

[24] L.-G. Xu, W. Ma, L.-B. Wang, C.-L. Xu, H. Kuang, N. A. Kotov, *Chem. Soc. Rev.* **2013**, *42*, 3114-3126.
[25] a) W. D. Knight, K. Clemenger, W. A. Heer, W. A. Saunders, M. Y. Chou, M. L. Cohen, *Phys. Rev. Lett.* **1984**, *52*, 2141-2143; b) M. Walter, J. Akola, O. Lopez-Acevedo, P. D. Jadzinsky, G. Calero, C. J. Ackerson, R. L. Whetten, H. Groenbeck, H. Hakkinen, *Proc. Natl. Acad. Sci. USA.* **2008**, *105*, 9157-9162.
[26] J. U. Reveles, S. N. Khanna, P. J. Roach, A. W. Castleman, *Proc. Natl. Acad. Sci. USA.* **2006**, *103*, 18405-18410.
[27] A. Fernando, K. L. Dimuthu, M. Weerawardene, N. V. Karimova, C. M. Aikens, *Chem. Rev.* **2015**, *115*, 6112-6216.
[28] H.-Y. Yang, J.-Z. Yan, Y. Wang, G.-C Deng, H.-F. Su, X.-J. Zhao, C.-F. Xu, B.-K. Teo, N.-F. Zheng, *J. Am. Chem. Soc.* **2017**, *139*, 16113-16116.
[29] a) K. Kwak, Q. Tang, M. Kim, D. E. Jiang, D. Lee, *J. Am. Chem. Soc.* **2015**, *137*, 10833-10840; b) P. R. Nimmala, B. Yoon, R. L. Whetten, U. Landman, A. Dass, *J. Phys. Chem. A* **2013**, *117*, 504-517; c) X. Kang, S. Chen, S. Jin, Y.-B. Song, Y.-J. Xu, H.-Z. Yu, H.-T. Sheng, M.-Z. Zhu, *ChemElectroChem* **2016**, *3*, 1261-1265.

Entry for the Table of Contents

RESEARCH ARTICLE

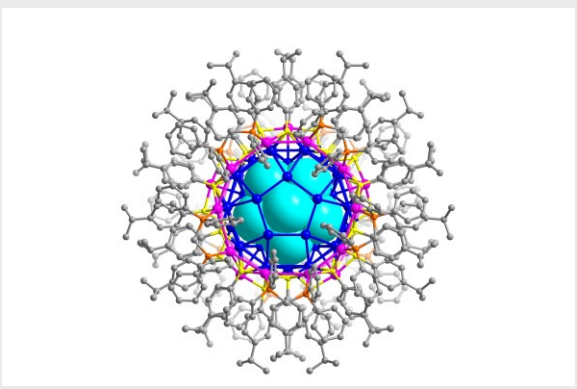

SD/Ag78a shows a core-shell structure comprised of an all-metallic Ag_{53} kernel surrounded by an Ag_{25} discontinuous metal-organic shell. Three types of ligands of thiol, phosphine and chloride regioselectively ligate on the surface of the Ag_{78} nanocluster.

*Wen-Jing Zhang, Zhen Liu, Shan-Shan Zhang, Ke-Peng Song, Christine M. Aikens, Zhi Wang, Chen-Ho Tung, and Di Sun**

Page No. – Page No.

A 34-Electron Superatom Ag_{78} Cluster with Regioselective Ternary Ligands Shells and Its 2D Rhombic Superlattice Assembly